



Interpreting atomization of agricultural spray image patterns using latent Dirichlet allocation techniques

Hongfei Li ^a, Steven Cryer ^{b,*}, John Raymond ^b, Lipi Acharya ^b

^a Department of Statistics, University of Illinois at Urbana-Champaign, Champaign, IL, USA

^b Data Science, Corteva Agriscience, Indianapolis, IN, USA

ARTICLE INFO

Article history:

Received 30 January 2020

Received in revised form 24 October 2020

Accepted 25 October 2020

Available online 28 October 2020

ABSTRACT

Breakup patterns of agricultural formulations are explored using unsupervised learning techniques to elucidate the mechanics of atomization for oil-in-water formulations. Previous researchers have shown these formulations succumb to a different breakup mechanism than conventional formulations, beginning with inhomogeneities within the liquid sheet that nucleate holes within the material being sprayed, beginning the mechanism responsible for breaking the sheet into droplets. The Latent Dirichlet Allocation (LDA), a Bayesian hierarchical model, is used to explore unsupervised learning relationships between image analysis metrics on spray video data and the resulting atomization droplet size. Latent factors discovered by LDA were used for classification of video segments and achieved 99.9% accuracy (3-fold cross validation). Seventy-five videos were used for regression where each video had a unique measured droplet size distribution (D10, D50, and D90 values) for atomization. Experiments using the features learnt by Latent Dirichlet Allocation used with regression have extremely good results ($R^2 \sim 0.995$ in 3-fold cross validation, $R^2 \sim 0.963$ on never-seen videos), which serves as evidence for the potential use of this model in image analysis of agricultural spray patterns. LDA has huge potential in both learning and predicting atomization patterns [e.g., driftable fines (drops $< 150 \mu\text{m}$)] when used with images based on the breakup phenomena in agricultural spray. These small drop sizes that occur during atomization have the greatest propensity for off-target movement through wind induced drift. LDA proved useful in characterizing current and future formulation designs using only images as witnessed by observations and excellent predictions summarized in this paper. In fact, these methods offer potential for use under field conditions to address spray performance based upon images of spray patterns at the nozzle without the need for expensive light scattering equipment often used to measure this phenomenon.

© 2020 The Authors. Publishing services by Elsevier B.V. on behalf of KeAi Communications Co. Ltd. This is an open access article under the CC BY-NC-ND license (<http://creativecommons.org/licenses/by-nc-nd/4.0/>).

1. Introduction

Flat-fan and air-induction hydraulic nozzles, mounted on spray booms, are the primary tools used to deliver agrochemicals to their target location. Nozzles are mounted on delivery booms for both ground and aerial delivery systems. Pesticide mixtures being sprayed leave the nozzle and begin as a liquid sheet which fans outward from the nozzle and eventually breaks up into liquid drops. Instabilities decompose the sheet into droplets by a variety of likely mechanisms, a phenomenon known as spray atomization (Dorman (1952)).

Agrochemical spray drift is an increasingly important field of study due to increased environment stewardship, legal liabilities, and the indirect costs of off-target effects (Palardy and Centner, 2017; Moeller, 2018; Viera et al., 2019). The resulting drop size greatly influences how well the sprayed chemical is delivered to the target. The ultimate size of the drops dictates both efficacy and potential off target

movement (e.g., drift). Attempts at the mechanistic understanding phenomena of spray drift can be found elsewhere (Squire, 1953; Barlow et al., 2011; Altieri et al., 2014; Cryer and Altieri, 2017; Altieri and Cryer, 2018).

Atomized drop size greatly influences the chemical effectiveness when delivered to its target. Large (coarse) drops may not effectively cover the target or may bounce upon impact with foliage. This is contrasted by smaller drops that risk becoming entrained in ambient air currents and carried off target, known as droplet drift. These small drops that are susceptible to off target movement are known as driftable fines. Driftable fines is not a standardized quantity but it is on the order of drop diameters $\leq 150 \mu\text{m}$ (Cloeter et al., 2010).

Experimental observations for spray patterns for multiphase emulsions are also reported (Li et al., 2020; Altieri et al., 2014) and used for comparison and training in unsupervised learning techniques. Latent Dirichlet Allocation (LDA) models are used in this analysis which differ from deep learning approaches and constitute a generative statistical model that allows sets of observations to be explained by unobserved groups that elucidate why parts of the data are similar.

* Corresponding author.

E-mail address: steven.cryer@corteva.com (S. Cryer).

2. Methods and materials

2.1. Data

The droplet size distribution emanating from the nozzle was obtained using a Sympatec laser diffraction system shown in Fig. 1 (Fritz and Hoffmann, 2016). This liquid sheet area, from the nozzle tip to the distance where the sheet breaks up into drops, was imaged by video.

Spray images videos were taken by a high-speed camera (Photron® Fastcam SA3 high-speed camera and a Nikon ED AF Nikkor® 80–200 mm lens) with 1024×1024 pixels resolution at 2000 frames per second.

The dataset consists of 83 videos belonging to 44 classes. Videos of the same class are recordings of repeated trials with exactly the same formulations, pressure and nozzles. Each video contains around 3000 frames and a total of 263,951 frames were obtained across all videos. Since videos were taken at different times with different nozzles, shape, size, and position of nozzles as well as brightness of images could change. To standardize those videos, every frame was preprocessed. Nozzles and headers at the top of each frame were aligned and then cropped from each image frame. The background of the centered spray patterns was denoised. Finally, each frame was turned into gray-scale fooled by conversion into black-and-white only (i.e. intensity of a pixel is either 0 or 255) since intensity variance is not relevant in our case. Example of a standardized frame is provided in Fig. 2 (b) along with the raw frame in Fig. 2 (a).

2.2. Latent Dirichlet allocation

Deep learning models using the same dataset are reported in Li et al. (2020). Better overall performance is anticipated when using averaging methods if models are uncorrelated. Latent Dirichlet Allocation Models differ from deep learning approaches, constituting a generative statistical model that allows sets of observations to be explained by unobserved groups that elucidate why some part of the data are similar. LDA was first introduced for natural language processing by Blei et al.

(2003). It is a three-level hierarchical Bayesian model, in which each item of a collection is modeled as a finite mixture over an underlying set of topics, and each topic is modeled as an infinite mixture over an underlying set of topic probabilities. A graphic model of LDA is showed in Fig. 3. Here, plate notation is a method of representing variables that repeat in a graphical model in Bayesian inference. A plate (or rectangle) is used to group variables into a subgraph that repeat together, and a number is drawn on the plate to represent the number of repetitions of the subgraph in the plate.

According to Blei et al. (2003), an easy way to understand LDA is to look at the processes it assumes for each document within a document-term matrix (e.g., corpus).

1. Choose $N \sim \text{Poisson}(\xi)$
2. Choose $\theta \sim \text{Dir}(\alpha)$
3. For each of the N words w_n :
 - a. Choose a topic $z_n \sim \text{Multinomial}(\theta)$
 - b. Choose a word w_n from $p(w_n|z_n, \beta)$, a multinomial probability conditions on the topic z_n .

To put it simply, topics are distributions over words, and documents are distributions over topics. Suppose we have information from many documents that talk about news on different topics such as social, sport, finance, politics, etc. Some words (e.g. football, win, score) are more likely to appear in sport news than financial news. It is natural to assume that, each topic consists of different set of words, or more accurately, each topic corresponds to a different probability distribution of words. Moreover, a document might contain several topics such as news that talks about an event that is related to both finance and law. LDA captures this by assuming each document corresponds to a combination of topics (e.g., 20% political, 50% financial, 30% social, and so on).

An image can also be treated as a document when it comes to image processing. For example, an image of a natural scene is a document. This scene may consist of 30% sky, 20% sea, and 50% sand, where sky, sea, and sand are topics. The topic sky might assign higher probability to visual

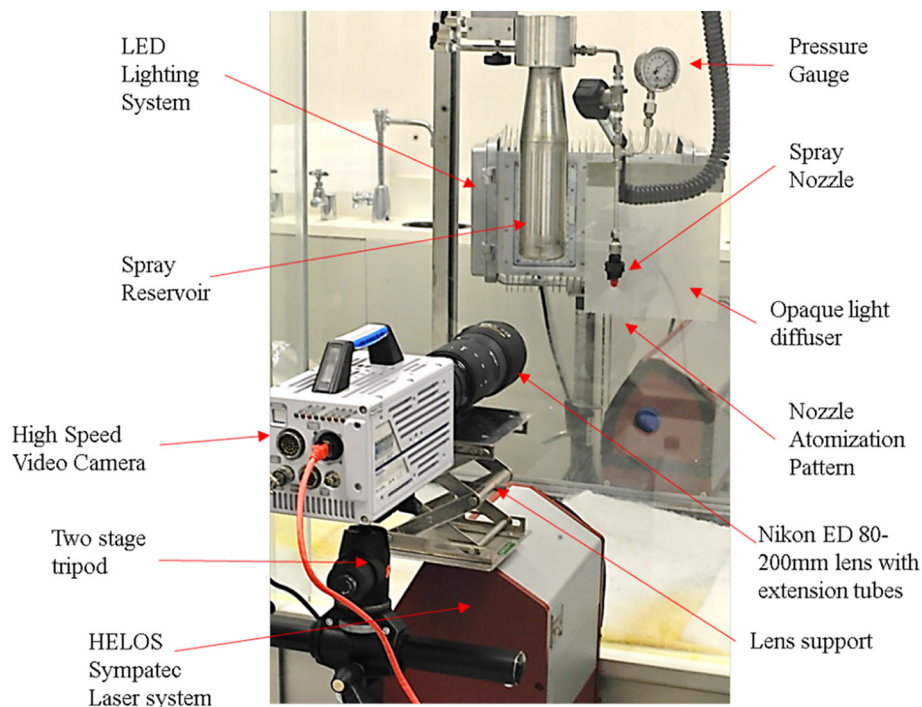


Fig. 1. The experimental spray chamber, nozzle system, Sympatec laser, and high-speed video camera used to measure the atomization drop size distribution and imaging the spray sheet. Experimental setup at Corteva Indianapolis site.

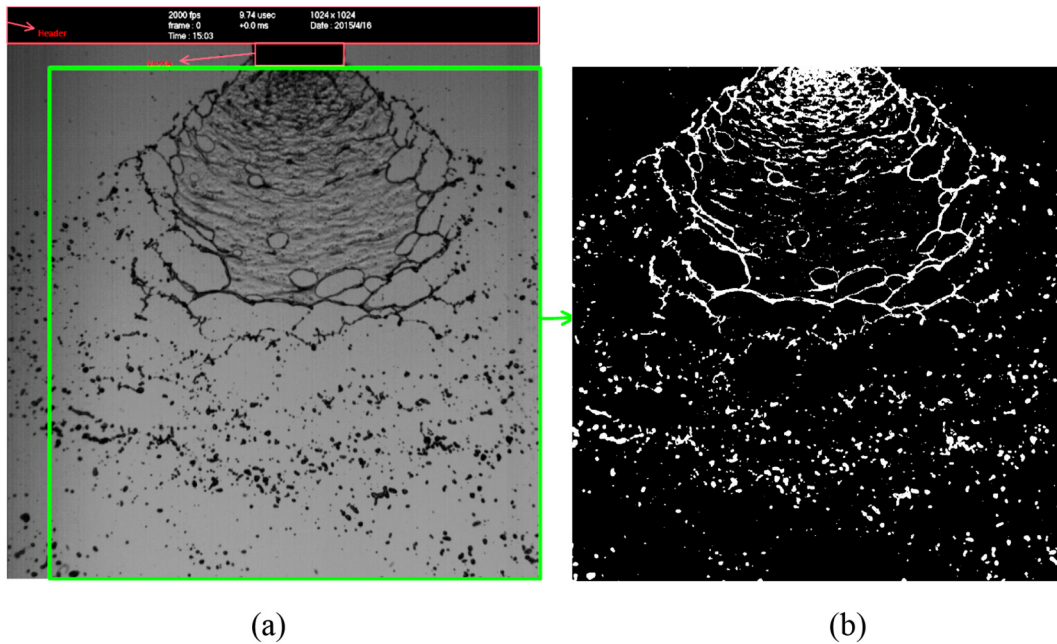


Fig. 2. Single raw frame example extracted from a video showcasing the header and nozzle requiring removal (red boundary) and centering image (green boundary) (a), followed by denoising and conversion to a black-and-white only image (b).

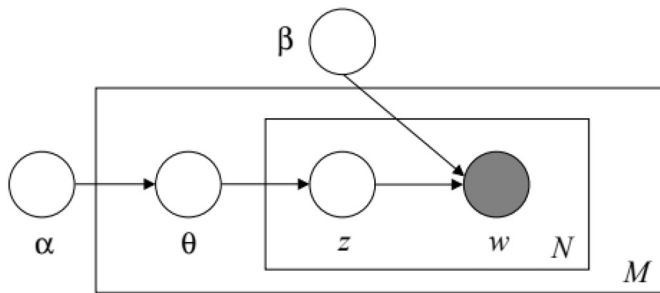


Fig. 3. Latent Dirichlet Allocation graphic model (taken from Blei et al. (2003)). Nodes are random variables where shaded nodes are observed and unshaded ones are unobserved. The plates indicate repetitions. The outer plate represents documents, while the inner plate represents the repeated choice of topics and words within a document.

words that are white or blue, while the topic sand might assign higher probability of visual words that are yellow.

As a result, although originally a language model, LDA has been brought into and widely used in computer vision. Applications of LDA include object recognition (Sivic et al., 2005; Fei-Fei and Perona, 2005; Russell et al., 2006; Cao and Fei-Fei, 2010), natural scene classification (Fei-Fei and Perona, 2005), human action classification (Niebles et al., 2008), activity perception in complicated scene (Wang et al., 2007), etc. Variants of LDA were developed for different tasks such as Spatial LDA (Wang and Grimson, 2008) for capturing spatial structures and Correspondence LDA (Blei and Jordan, 2003) for image annotation. In this work, we apply LDA to spray pattern images to obtain interpretable underlying features that can be subsequently used in supervised learning tasks.

2.3. Feature construction

2.3.1. Bag of words

Words, vocabulary, and documents are required to apply LDA. Thus, *visual words* are extracted (which are local areas of images) in handling

image data. For example, in natural scenes, there is likely to be stones, mountains, sky, sun, trees, and so on. These objects are characterized as visual words, and they form the vocabulary of natural scenes. Fei-Fei and Perona (2005) sample local regions from images by several methods (including evenly grid sampling) and use a k-means algorithm to cluster these local regions to get the vocabulary. In this way, a local region of an image corresponds to a word, and an image, which is a collection of words, becomes a document. Other approaches employ the use of super-pixels to over-segment images in regions of related pixels (Chen et al., 2017; Qiaojin et al., 2011).

A video is a sequence of images, and in some cases human action recognition (e.g., spatial-temporal information) is critical. Niebles et al. (2008) represented each video sequence as a collection of spatial-temporal words by extracting space-time interest points. However, human actions are highly structured and non-random, while the spray videos consist of random, unstable image textures, white dots and lines. Static instances of an image spray pattern textures are insufficient to properly categorize the information content of such dynamic, highly random phenomena. It is the temporal distribution of these image texture regions over the course of a video stream that provide discriminability. Thus, we treat videos as bags of visual words. Each frame is an unordered collection of visual words, and sequence of frames are still an unordered collection of visual words. A sequence of frames are the collections of all visual words that appear in any of these frames. We count how many times a word appears in a document, and a document is then represented by the counts of words (known as a document-word matrix). A bag-of-words model is often used in document classification where the frequency of occurrence for each word is a feature for training a classifier (McTear et al., 2016; Harris, 1954).

For example, suppose we have two documents. The first document is “James likes apples and Emma likes oranges.” And the second one is “James hates oranges.” We can represent the two documents as two bags of words (BoW):

BoW1 = {“James”:1, “likes”:2, “apples”:1, “and”:1, “Emma”:1, “oranges”:1};

BoW2 = {“James”:1, “hates”:1, “oranges”:1};

and the document-word matrix is constructed as follows:

	James	likes	hates	apples	and	Emma	oranges
Document1	1	2	0	1	1	1	1
Document2	1	0	1	0	0	0	1

2.3.2. Codebook

Similarly, we can construct a document-word matrix for images by thinking of an image as a document and local regions of an image as words. We cut images into small local regions, use k-means to get a dictionary of visual words, and then form a bag of words representing a sequence of images. All images are downsampled to 500×500 pixels for LDA. Each image is cut into 10×10 pixels small patches and we remove all patches that are completely empty (i.e., if every pixel in a patch is 0, it contains the black background only).

Fifteen hundred frames are randomly sampled (due to memory limitations and the relative simplicity of the elements in our images) to perform k-means. A vocabulary size of 200 is selected (i.e., 200 cluster centers for the k-means) and we get a dictionary containing 200 visual words of our “language” following the k-means step. We also obtain another 50 visual words using pyramid features extraction method

described in section 2.3.3. Fig. 4 illustrates the codebook that is learned from the frames, and we use the 250 visual words in the codebook to describe the images. We assign each local patch sampled from a frame to the visual word that is most similar. In this way, an image becomes a bag of visual words from the codebook.

2.3.3. Pyramid features

Since we resize each frame to 500×500 pixels and sample 10×10 pixels local patches from these frames, each patch contains a very small portion of information in the original frame. One patch might contain a dot or part of a line (i.e., a very low-level feature about the image). However, we would also like to have features that describes higher level information about the image, (such as the spray angle of sheets), and we adopt the feature extraction method used by Lazebnik et al. (2006). After we extract local patches from 500×500 pixels images, we shrink each image to 100×100 pixels and cut them into 10×10 pixels local patches again. In this way, one patch can contain more information in relation to the size of the image (i.e., higher-level features such as the angle of sheets in addition to a dot or a short line).

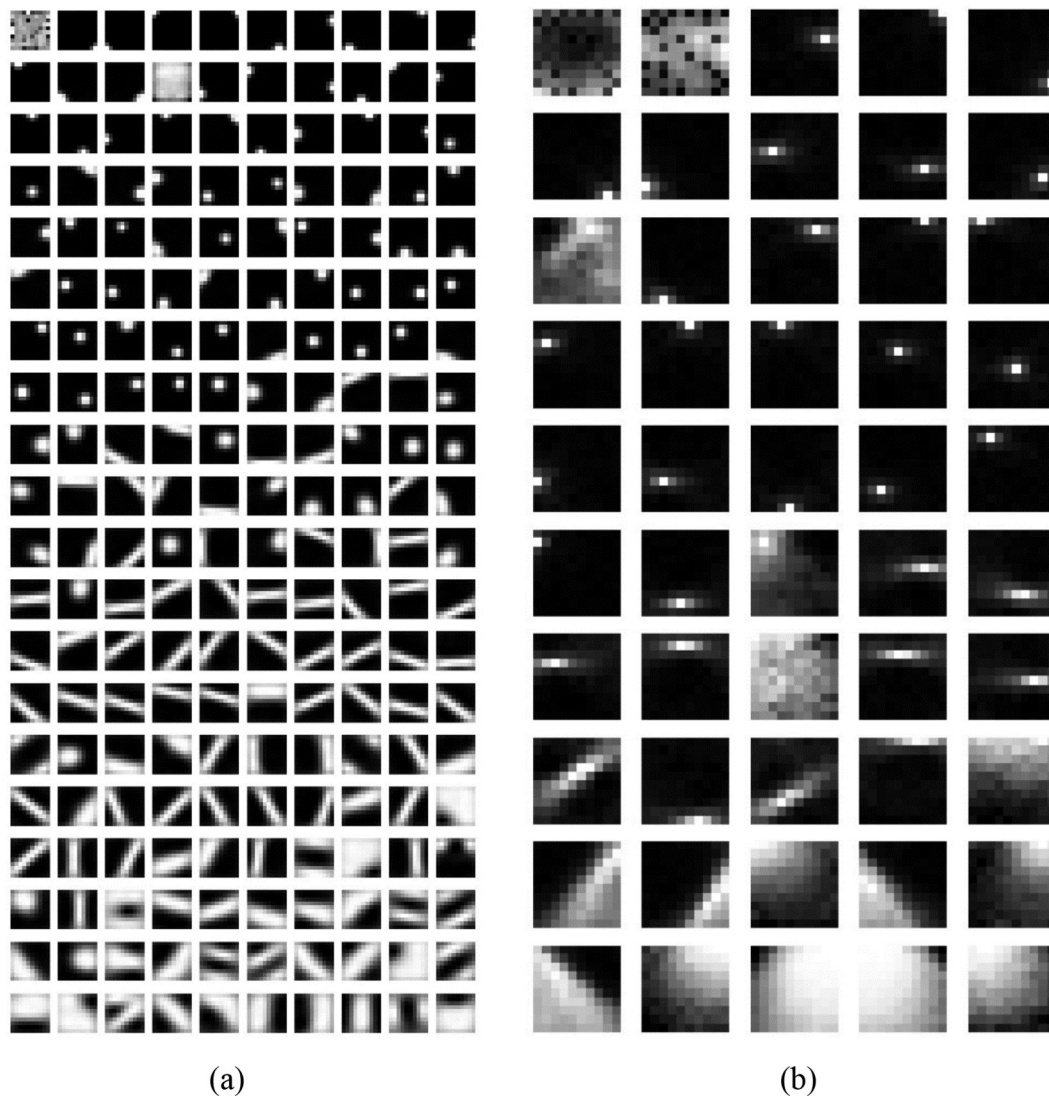


Fig. 4. Codebooks sorted by frequencies. Left (a) is the codebook with 200 low level visual words. Right (b) is the codebook with 50 high level visual words.

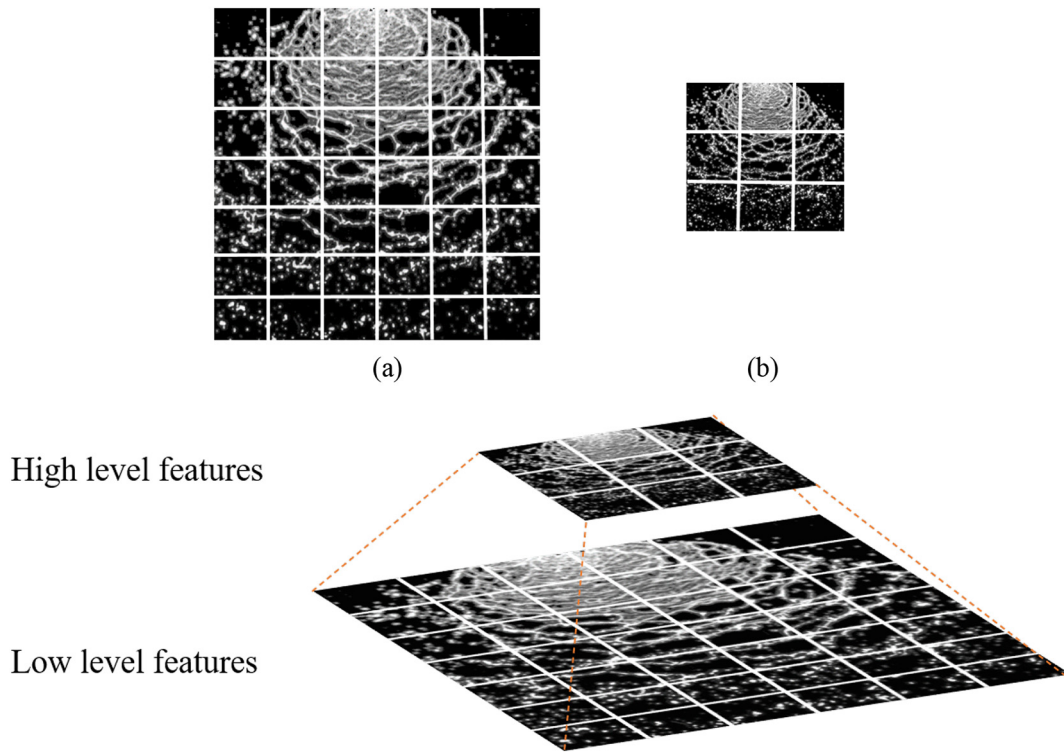


Fig. 5. Pyramid features extraction. Low level patches (a) from high resolution images of atomization process. High level patches (b) from low resolution images.

Fig. 5 illustrates the approach of extracting spatial pyramid features from an image of spray emanating from a nozzle in order to obtain our

codebook of high-level visual words (right side, Fig. 4). We extract low-level features from high-resolution images and extract high-level

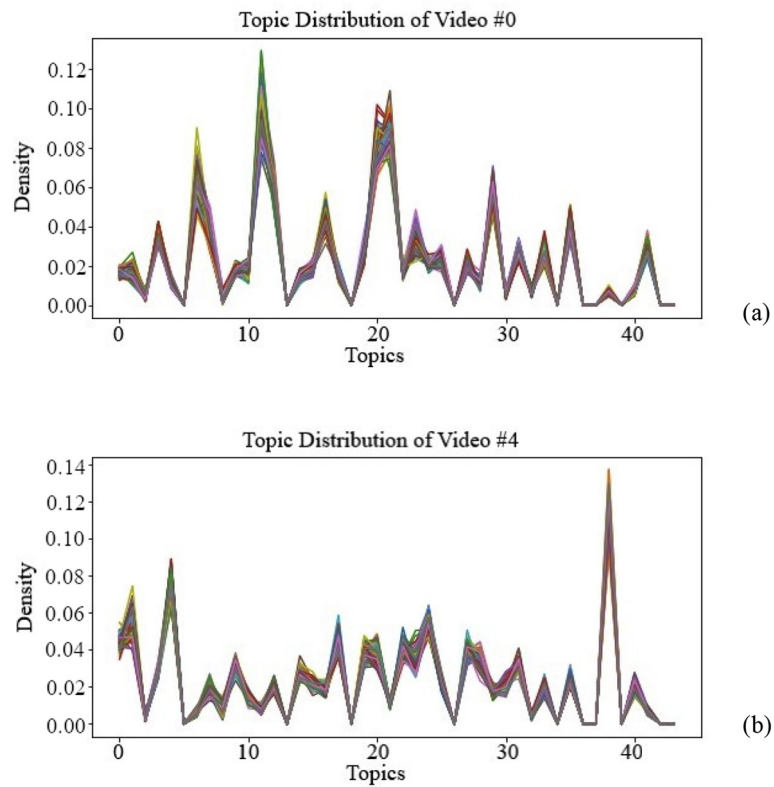


Fig. 6. Topic proportion of four example videos. Each subplot is a video that consists of many video segments. Each line in the plot is the topic proportion of a video segment. The top (a) and bottom (b) video each belongs to different classes.

features from low-resolution images. We fit other k-means to these higher-level patches, and learn a new codebook, where the vocabulary size is selected as 50. These 50 words and the previous 200 words consists of the complete vocabulary of size 250. Every frame is turned into a bag of these visual words. Each word is counted to construct the document-word matrix.

3. Results

3.1. Clustering results and insights

Data consists of 83 high speed videos belonging to 44 classes (where most classes contain two videos). Most videos contain around 3000 frames. Each frame is transformed into black-and-white image. We split each video into smaller video segments where each video segment consists of 25 consecutive frames. We treat a video segment as a document (instead of a frame as a document) where most videos contain around 100 video segments. Most frames sizes are approximately 1000×1000 pixels, but we resize them into 500×500 pixels.

The dataset is split randomly into a small training set (for learning the codebook) and a test set.

Approximately 200 low level visual words and 50 high level visual words are learned in training. We set the number of topics of the Latent Dirichlet Allocation model as 44. Although we use same number of

topics as classes, we do not expect one-to-one correspondence between topics and classes. Usually, a class is defined by multiple dominant topics.

The unnormalized topic proportion for each document, or video segment, is obtained after fitting the Latent Dirichlet Allocation model. A class is defined by its unique topic proportions, and this topic proportion is used to analyze similarity and difference between classes. The topic proportion for two example videos is provided in Fig. 6. Each line in the plot is the topic proportion of a video segment. Each subplot contains video segments that come from the same video. We can see that video segments that come from the same video have very similar topic proportions. A video class represents the formulation attributes that lead to how the material breaks up into droplets and the resulting drop size. And the topic proportion of video segments of this class are almost the same. The top and bottom video each belongs to different classes, Fig. 6. Thus, the topic proportions are different.

The top two principle components (PCA) of topic proportion of each video segment are represented in Fig. 7, with different colors indicating different classes. PCA produces a low-dimensional representation of a dataset by finding a sequence of linear combinations of the variable having maximum variance that are mutually uncorrelated and serves as a tool for data visualization. A dot is a video segment. A cloud is a video. From Fig. 7, one sees that video segments of the same class are mostly grouped together.

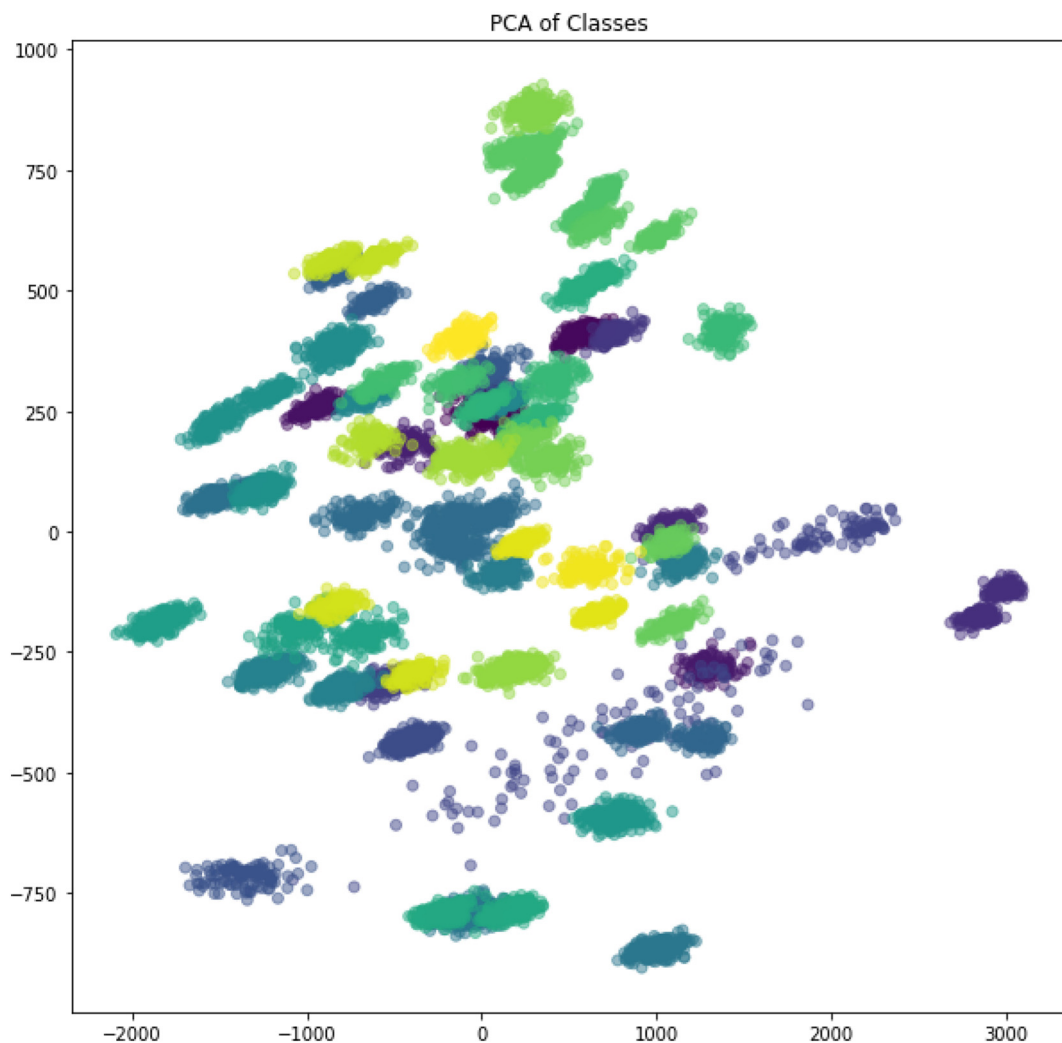


Fig. 7. Principle Components Analysis of topic proportion of each video segment using the first two principle components. A dot is a video segment. A cloud is a video. Different color indicating different classes.

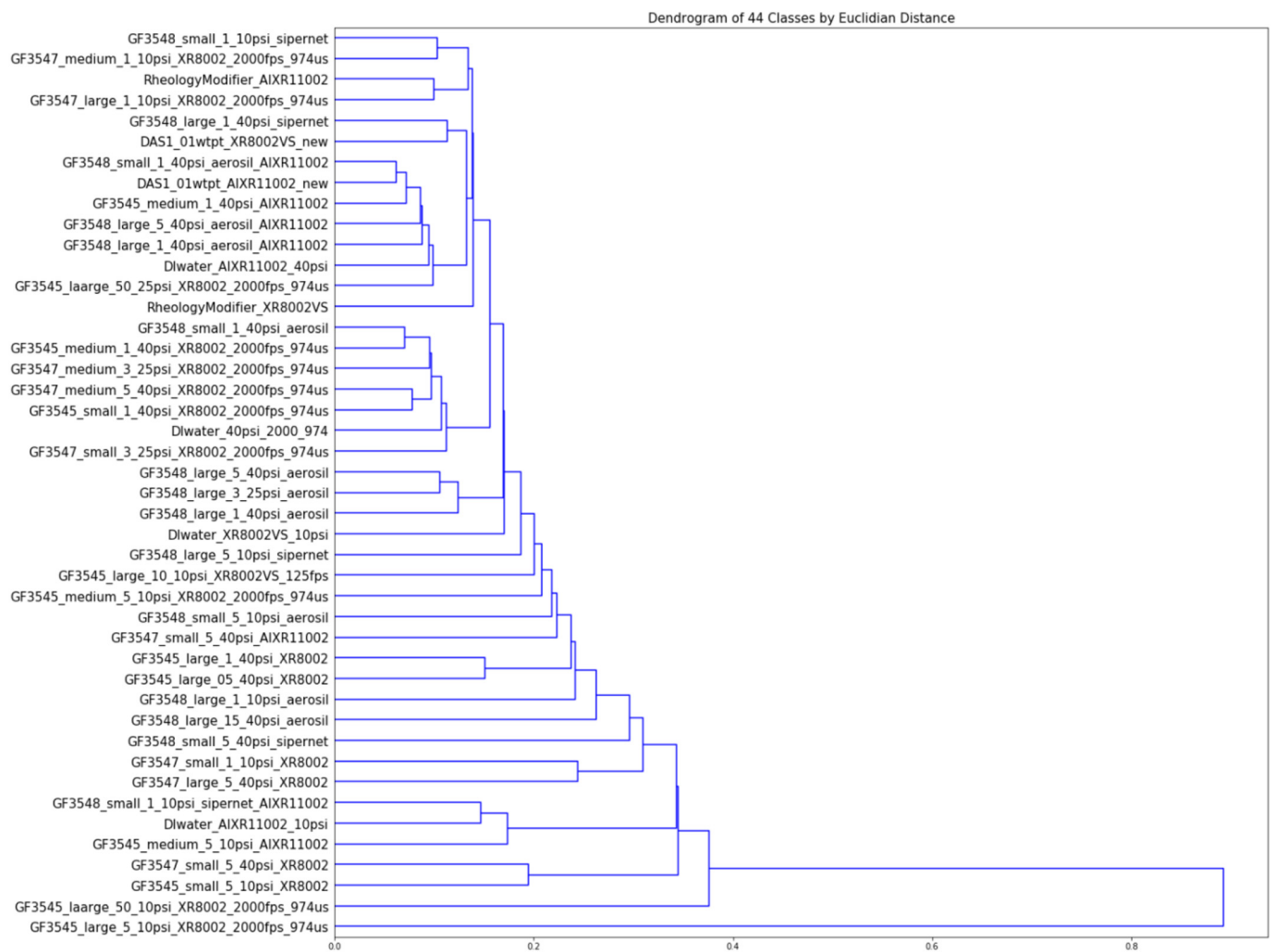


Fig. 8. Dendrogram of classes by Euclidian distance of their topic proportions.

Fig. 8 shows the dendrogram of classes by Euclidian distance of their topic proportions (i.e., a tree diagram used to illustrate the arrangement of the clusters produced by hierarchical clustering). A dendrogram is useful to explore the numbers of various clusters that form between different video classes with similar formulations clustering close to one another. However, often dramatically different formulations can cluster together (similar results for PCA).

Topics are distributions over words and one can further examine what these topics are. A crude idea of topic descriptions is determined by looking at the high frequency words of a certain topic. In Fig. 9, the majority of first topic is dots, while polygons, or holes, appear in the second topic more frequently. The third topic is about vertical lines, and the last example shows lines of different orientations. If a class has a high proportion of the first topic and low proportion of the last topic, there might be more dots than lines in the videos of this class.

3.2. Video segment classification

Latent Dirichlet Allocation discovers the topic distribution which define classes in an unsupervised fashion. Each class has a unique topic proportion. Supervised models can be built if topic proportions are taken as a feature vector that describes each class. Linear Discriminant Analysis is chosen to perform classification using topic distributions. There is a total of 10,461 video segments, 83 videos, 44 classes for the spray atomization videos. Video segments originating from the same

video share the same class label. Unique classes represent video observations that yield similar behavior.

The topic proportion of each video segment is used as its features. Even when running videos at steady state, the dynamic nature for the fluid sheets suggest that it is possible for video segments to be misclassified into different classes depending upon where in the process the video segments is taken. Thus, the dataset is first split into training and testing sets by video segments (i.e., 2/3 of all video segments are train data, 1/3 of all video segments are test data). A Linear Discriminant Analysis model is trained via the training set, and predictions for the class of video segments (25 frames) are analyzed in the test set. Accuracy of 3-fold cross validation is 99.9%. Table 1 shows the high cross-validation accuracy of the classification for this approach. A possible explanation to the high accuracy may be due to having multiple video segments for a single video.

For further insights into generalizability of these features, the dataset is then split into train and test set by videos. There are 31 classes containing two or more different videos. For those classes, video segments coming from one video are in train set, and video segments coming from another video are in test set. This approach results in 5742 video segments in train set and 4719 video segments in test set. Again, a Linear Discriminant Analysis model is used to classify these video segments, and it achieved 85.9% accuracy.

Table 1 summarizes the classification results. The high classification accuracy shows that the topic distributions extracted by Latent Dirichlet

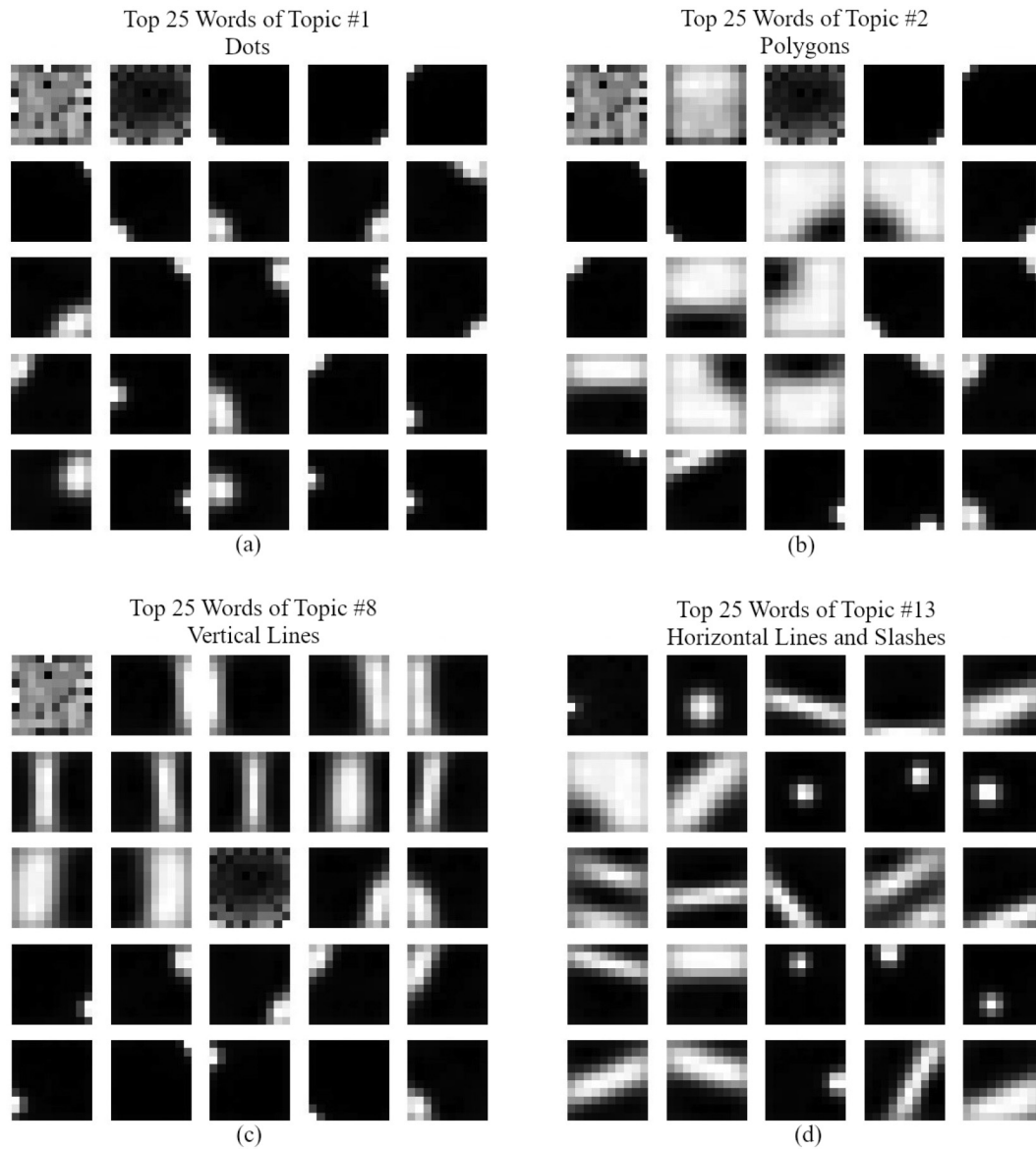


Fig. 9. Top 25 words of 4 example topics. Topic in (a) mostly consists of dots. Topic in (b) consists of polygons and holes. Topic in (c) consists of vertical lines and dots. Topic in (d) consists of horizontal lines, slashes and dots.

Allocation successfully captured and summarized each video segment and proved to be good features for classification.

3.3. Drop size prediction

Feature vectors are also used to do regression in addition to classification. Only 75 of the 83 videos utilized for Latent Dirichlet Allocation had atomization drop size distributions summarized for three measurements (i.e., D10, D50, and D90 values representing drop size particle diameter corresponding to 10, 50 and 90% cumulative), leaving 9621 video segments (75 videos) for the regression task. The independent

variables are the topic proportion of each video segments (smaller subset of main video) and are different for each video segments (although the difference is extremely small if two video segments are derived from the same video). The dependent variables are the three measurements, D10, D50, and D90.

Data is split into a train and test set by video segments (e.g., 2/3 of all the video segments are train data, and 1/3 of all video segments are test data). A polynomial regression with degree 2 is fit to the train set and make predictions on test set. Table 2 summarizes the result. The average

Table 1
Classification accuracy with Linear Discriminant Analysis.

Split method	Average classification accuracy
3-fold cross validation by video segments	99.9%
Split by videos	85.9%

Table 2
Drop Size Prediction.

Model	Mean squared error	Explained variance
Latent Dirichlet Allocation + Polynomial Regression (3-fold CV)	51.6	99.5%
CNN + RNN (Li et al., 2020)	39.5	99.6%

R-squared value is 99.5% for a 3-fold cross validation. We also list the result of a deep learning regression model that uses the same videos and D10, D50, D90 data reported earlier for comparison (Li et al., 2020). The train-test split ratio is 2:1 for both models.

In addition, similar to video segment classification, the dataset is also split into train and test sets by videos, where video segments coming from the same video are either in train set or test set. This approach results in 5550 video segments in train set and 4071 video segments in test set. A polynomial regression with degree 2 is used, mean squared error of test set is 361.2, and R-squared value of test set is 96.3%.

4. Conclusions

The mechanism for delivering many pesticides to the target site is by atomization of spray using hydraulic nozzles. Atomization shows rich diversity and is a function of formulation type, composition, the number of phases within the formulation, spray pressure, nozzle geometry, and so on. Breakup patterns from spray nozzles are explored using unsupervised learning techniques to elucidate the mechanics of atomization for oil-in-water formulations. The Latent Dirichlet Allocation (LDA), a Bayesian hierarchical model, is used to perform unsupervised learning on video spray data for agricultural formulations. The LDA model discovers and learns about the latent factors for the data to provide insight on information that is much more interpretable than that obtained via black box methods. Latent factors discovered by LDA were used for supervised learning tasks including classification and regression.

A Linear Discriminant Analysis model was able to classify video segments with 99.9% accuracy (3-fold cross-validation) based on those latent factors. Seventy-five videos were used for regression where each video had a unique measured droplet size distribution (D10, D50, and D90 values) for atomization. The primary experiments using the features learnt by Latent Dirichlet Allocation used with regression (3-fold cross-validation) have extremely good results ($R^2 \sim 0.995$). Further experiments where never-before-seen videos were held out as test set still give good results ($R^2 \sim 0.963$), which serves as evidence for the potential use of this model in image analysis of agricultural spray patterns. The Latent Dirichlet Allocation model offers huge potential to learn and predict atomization patterns (e.g., especially driftable fines) when used with images based on the multiphase breakup phenomena witnessed in agricultural spray drift. Small drops of sizes $<150 \mu\text{m}$ offer the greatest propensity for off-target movement via wind induced drift, and LDA methods can be used to offer insight into the drop sizes manifest with spraying oil-in-water formulations. Images can be obtained from videos obtained in spray chambers (this work) or from real time videos of spray phenomena at the source along a boom in field applications. Thus, process control can come into play to keep drop sizes within a targeted range (e.g., spray performance).

Author Statement

Hongfei Li was a principle author involved in all aspects of this work. She was a Master's Student in Statistics at the University of Illinois Urbana Champaign at the time of this work. Hongfei was supervised by Lipi Acharya and Steven Cryer of Corteva Agriscience (Data Science and Informatics) when she was finishing her Master's degree at UIUC. Dr. Acharya and Dr. Cryer provided the necessary ideas, support, feedback, guidance, and interactions for this work. Dr. John Raymond of Corteva Agriscience also provided technical guidance.

Declaration of Competing Interest

No conflict of interest exists.

Acknowledgements

Dr. Navin Elango provided critical review and feedback of this manuscript. Hongfei Li was a master's student at the University of Illinois, Urbana-Champaign (UIUC) working with Corteva Agriscience as an intern at the time this work was undertaken. All research was funded by Corteva Agriscience.

Appendix A. Supplementary data

Supplementary data to this article can be found online at <https://doi.org/10.1016/j.aiia.2020.10.004>.

References

- Altieri, A.L., Cryer, S.A., 2018. Break-up of sprayed emulsions from flat-fan nozzles using a hole kinematics model. *Biosystems Engineering* 169, 104–114.
- Altieri, A., Cryer, S.A., Acharya, L., 2014. Mechanisms Experiment and Theory of Liquid Sheet Breakup and Drop Size from Agricultural Nozzles. *Atomization and Sprays* 24 (8), 695–721.
- Barlow, N.S., Helenbrook, B.T., Lin, S.P., 2011. Transience to instability in a liquid sheet. *J. Fluid Mech.* 666, 358.
- Blei, D.M., Jordan, M.I., 2003. Modeling annotated data. *Proceedings of the 26th annual international ACM SIGIR conference on Research and development in information retrieval*, pp. 127–134.
- Blei, D.M., Ng, A.Y., Jordan, M., 2003. Latent dirichlet allocation. *J. Mach. Learn. Res.* 3 (4–5), 993–1022.
- Cao, L., Fei-Fei, L., 2010. Spatially coherent latent topic model for concurrent object segmentation and classification. *Proceedings of IEEE Intern. Conf. in Computer Vision (ICCV)*, p. 2010.
- Chen, C., Zare, A., Trinh, H.N., Omotara, G.O., Cobb, J.T., Lagaunne, T.A., 2017. Partial Membership Latent Dirichlet Allocation for Soft Image Segmentation. *IEEE Transactions on Image Processing* 26 (12), 5590–5602.
- Cloeter, M.D., Qin, K., Patil, P., Smith, B., 2010. Planar Laser Induced Fluorescence (PLIF) flow visualization applied to agricultural spray nozzles with sheet disintegration; Influence of an oil-in-water emulsion. *ILASS Americas 22nd Annual Conference on Liquid Atomisation and Spray Systems*, Cincinnati, OH, May 2010.
- Cryer, S.A., Altieri, A.L., 2017. Role of large inhomogeneities in initiating liquid sheet breakup in agricultural atomization. *Biosyst. Eng.* 1693, 103–115.
- Dorman, R.G., 1952. The atomization of liquid in a flat spray. *Br. J. Appl. Phys.* 3, 189.
- Fei-Fei, L., Perona, P., 2005. A bayesian hierarchical model for learning natural scene categories. *Computer Vision and Pattern Recognition, CVPR 2005. IEEE Computer Society Conference*. 2, pp. 524–531.
- Fritz, B.K., Hoffmann, W.C., 2016. Measuring Spray Droplet Size from Agricultural Nozzles Using Laser Diffraction. *J. Vis. Exp.* 115, e54533. <https://doi.org/10.3791/54533>.
- Harris, Z., 1954. Distributional structure. *Word* 10 (23), 146–162.
- Lazebnik, S., Schmid, C., Ponce, J., 2006. Beyond bags of features: Spatial pyramid matching for recognizing natural scene categories. *2006 IEEE computer society conference on computer vision and pattern recognition (CVPR'06)*. 2, pp. 2169–2178.
- Li, H., Cryer, S., Acharya, L., Raymond, J., 2020. Video and image classification using atomisation spray image patterns and deep learning. *Biosyst. Eng.* 200, 13–22.
- McTear, M.F., Callejas, Z., Griol, D., 2016. The conversational interface, talking to smart devices. 6, no. 94. Springer, Cham, p. 102.
- Moeller, D.L., 2018. Superfund, pesticide regulation, and spray drift: rethinking the Federal Pesticide Regulatory Framework to provide alternative remedies for pesticide damage. *Iowa L. Rev.* 104, 1523.
- Niebles, J.C., Wang, H., Fei-Fei, L., 2008. Unsupervised learning of human action categories using spatial-temporal words. *Int. J. Comput. Vis.* 79 (3), 299–318.
- Palardy, N., Centner, T.J., 2017. Improvements in pesticide drift reduction technology (DRT) call for improving liability provisions to offer incentives for adoption. *Land Use Policy* 69, 439–444.
- Qiaojin, G., Ning, L., Yubin, Y., Ganghan, W., 2011. Supervised LDA for Image Annotation. *2011 IEEE international conference on systems, Man, and Cybernetics*.
- Russell, B.C., Freeman, W.T., Efros, A.A., Sivic, J., Zisserman, J.A., 2006. Using multiple segmentations to discover objects and their extent in image collections. *2006 IEEE Computer Society Conference on Computer Vision and Pattern Recognition (CVPR'06)*. Vol. 2, pp. 1605–1614.
- Sivic, J., Russell, B.C., Efros, A.A., Zisserman, A., Freeman, W.T., 2005. Discovering object categories in image collections. *Computer Science and Artificial Intelligence Laboratory Technical Report, MIT-CSAIL-TR-2005-012*, Feb 25 AIM-2005-005.
- Squire, H.B., 1953. Investigation of the instability of a moving liquid film. *Brit. J. Appl. Phys.* 4, 167–169.
- Viera, B.C., Luck, J.D., Amundsen, K.L., Gains, T.A., Werle, R., Kruger, G.R., 2019. Response of *Amaranthus* spp. following exposure to sublethal herbicide rates via spray particle drift. *PLoS one* 14 (7), e0220014.
- Wang, X., Grimson, E., 2008. Spatial latent Dirichlet allocation. *Adv. Neural Inf. Proces. Syst.* 20, 1577–1584.
- Wang, X., Ma, X., Grimson, E., 2007. Unsupervised activity perception by hierarchical bayesian models. *2007 IEEE conference on computer vision and pattern recognition. IEEE*, pp. 1–8.